

Laser patterning of metallic films via buffer layer

Gabriel Kerner, Micha Asscher *

Department of Physical Chemistry and the Farkas Center for Light Induced Processes, The Hebrew University, Jerusalem 91904, Israel

Received 21 November 2003; accepted for publication 19 February 2004

Abstract

A novel method is presented for a single pulse laser-patterning of variable width conducting lines on solid surfaces. Employing laser induced thermal desorption (LITD), potassium coverage grating on top of multilayer Xe is formed on Ru(001) at 20 K. Optical second harmonic-diffraction measurements were performed to characterize the grating as a function of Xe layer thickness and laser power density. Upon annealing to 80 K, the Xe layer desorbs and the metallic pattern softly lands on the substrate. The potential application of this procedure for the parallel writing of conducting wires millimeters long and less than 50 nm wide is discussed.

© 2004 Elsevier B.V. All rights reserved.

Keywords: Growth; Laser methods; Laser induced thermal desorption (LITD); Second harmonic generation methods; Second harmonic generation; Metallic films

1. Introduction

Nanometer size conducting wires and complex structures patterned over semiconductor, oxide and metallic substrates are currently at the forefront of modern technology. At the same time, basic scientific issues such as diffusion of adsorbates on surfaces [1–3], film growth mechanisms and molecular conductivity studies employing submicron metallic electrodes—all rely on spatial patterning of thin films. Periodic patterning of adsorbate coverage [1,2] has been demonstrated by means of laser induced thermal desorption (LITD) [4,5]. This method, while applicable for weakly bound adsorbates, may lead to surface damage in the case of strongly bound species. Species that

desorb above room temperature in most cases already require potentially damaging laser pulse energies. Consequently the formation of coverage grating of metal adsorbates directly bound to semiconductor or metallic substrate is practically impossible without causing surface melting or severe damage.

Metal deposition on surfaces via a homogeneous xenon buffer layer was proposed and developed by Weaver and coworkers [6–9]. This buffer layer assisted growth (BLAG) procedure was demonstrated to be a very efficient way to grow well defined metallic clusters on semiconductor surfaces. Similarly, xenon layer as a template for micrometer scale adsorbate patterning on surfaces was demonstrated by Williams et al. [10]. In this study, hydrogen atoms were selectively deposited over a xenon coverage grating on top of a Si(111) substrate that was prepared prior to hydrogen deposition, using the LITD technique.

* Corresponding author. Tel.: +972-2-5618033; fax: +972-2-5618033.

E-mail address: asscher@fh.huji.ac.il (M. Asscher).

In this work we introduce a novel method for metallic thin film patterning to form conducting wires that are millimeters long and can potentially be reduced to width of 50 nm or less. This is a highly versatile patterning method that can be employed practically with all elements and chemical species. The combination of LITD and BLAG methods mentioned above results in adsorbates coverage gratings that otherwise are impossible to form. These gratings enable, for example, macroscopic diffusion and sintering studies of low coverage metals on oxide surfaces, subject of growing interest in, e.g. catalysis related works in recent years [11–14]. The entire experimental setup was previously described [14,15], except for the ability to cool down to 20 K, added in this work by means of a closed cycle cryostat.

2. Results and discussion

A material that performs as buffer layer should interact weakly with the substrate and the metallic element on top. For example, multilayer xenon desorb from metallic surfaces in the range 45–70 K [16]. Using standard nanoseconds pulsed laser heating at a wavelength of 1064 nm, the corresponding peak temperature for the onset of

desorption is about 150 K. This temperature is calculated for absorbed laser power density of 2 MW/cm² (10 mJ/pulse). Employment of the buffer layer assisted patterning technique thus avoids the limitations of LITD with respect to strongly bound adsorbates. The fast heating associated with LITD of a Xe layer results in fast desorption, leading to buffer atoms ablation. In contrast, slow heating of an adsorbate covered physisorbed buffer layer leads to migration and “soft landing” of the adsorbate on the substrate, while the buffer layer evaporates, as discussed by Weaver and coworkers [6–9]. Another aspect of a buffer layer was pointed out by Cheng and Landman [17]. These authors described the function of the buffer layer as a cooling and stabilizing environment for metallic clusters evaporated on top.

A schematic view of our procedure for buffer layer assisted laser patterning of metallic grating is shown in Fig. 1. After sputter cleaning and annealing a substrate under UHV conditions, a layer of Xe is deposited on top at 20 K. A layer of the material to be patterned is then grown at an appropriate thickness. LITD coverage grating is then prepared in which Xe and the deposited material are removed in a single laser pulse at the constructive interference troughs of the laser grating. Finally, the remaining Xe is slowly heated

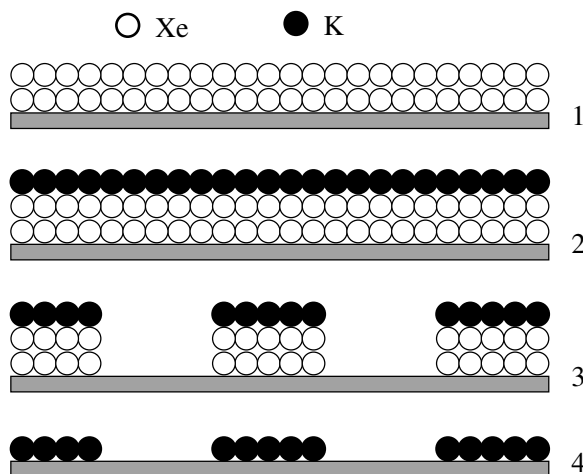


Fig. 1. A schematic view of the buffer layer assisted laser patterning procedure: (1) multilayer of a physisorbed buffer layer, (2) metal adsorption on top of the buffer layer, (3) spatial grating of the buffer together with the metal film via LITD, and (4) removal of the buffer layer by slow thermal annealing and “soft-landing” of the remaining adsorbate on the substrate.

and totally removed near 80 K. The deposited material gradually migrates to the substrate surface, retaining the pattern created on the Xe buffer layer.

As a model system we used metallic potassium on top of Xe over Ru(001) at 20 K under UHV conditions. Potassium is known for its high optical second harmonic (SH) response, therefore is suitable for in situ growth analysis, as was shown in our laboratory on Re(001) and Ru(001) [15,18,19]. At low coverage this element is strongly bound to metallic substrates (activation energy for desorption of 48 Kcal/mole was determined on Ru(001) at 0.3 ML, peak desorption near 650 K [15]). Our procedure, therefore, for low coverage LITD-grating formation of potassium, nicely demonstrates the unique ability of the buffer layer technique in patterning strongly bound metallic layers in general.

The vacuum system and experimental set-up in which this study has been performed were described elsewhere in detail [15,18]. Briefly, the Ru substrate was mounted on a cryogenic close cycle refrigerator (APD inc., minimum sample temperature 20 K), in a chamber at a base pressure of 1×10^{-10} mbar. Dosing of xenon and potassium was calibrated before and after each measurement by temperature programmed desorption (Δ P-TPD) and recording optical second harmonic response during TPD (SH-TPD). A p-polarized, 10 ns pulsed Nd:YAG laser at its fundamental wavelength of 1064 nm was used for both coverage grating formation via LITD and as the optical SHG probe beam. Periodic coverage modulations were created by overlapping two split beams of the same laser pulse on the sample surface, each beam is 50% of the original intensity at an incident angle of $\pm 6^\circ$ with respect to the surface normal. The resulting coverage grating had a period of 5 μm , at the dimensions of the laser beam, namely 6 mm diameter. A fraction of the fundamental laser beam used as the probe for SHG detection was limited to a power density of 0.1 MW/cm² in order to prevent any desorption of Xe from the surface by the SHG probe laser beam. The peak temperature rise due to the probe laser heating was calculated to be 18 K above the substrate temperature of 20 K. This is based on

standard heat diffusivity models used in LITD applications [4,5].

The SH signal from potassium evaporated on top of a xenon layer has been recorded. There is an overall SH intensity enhancement of about 30% by the xenon layer relative to the signal obtained from potassium on the bare Ru(001) surface, that is independent of the Xe layer thickness. Maximum SHG intensity was obtained for potassium coverage near 1 ML, consistent with the behavior of potassium directly deposited on Ru(001) [15] and other substrates [14,18–21]. In order to monitor the removal of potassium on top of Xe by the LITD process, single laser pulses were employed, at power densities in the range 0.3–3.5 MW/cm². These were conducted on samples containing 1 ML K on top of 60 ML Xe, as shown in Fig. 2. The remaining potassium coverage on top of the Xe layer following a single laser pulse that strikes the entire (6 mm) sample was monitored by running SH-TPD spectra. Integrated areas under such curves, when normalized to the signal at 1 ML, are used to evaluate the remaining potassium coverage [18]. Results are shown in the inset of Fig. 2. Such measurements were the basis for the choice of laser power densities best suited for the potassium coverage grating formation. This removal curve is a clear confirmation that the power densities used for the removal of the Xe buffer layer and potassium on top are well below those needed for desorbing a potassium layer directly attached to the substrate. For comparison, a minimum absorbed laser power density of 10 MW/cm² was necessary to obtain a rather shallow coverage grating of 1 ML potassium on Ru(001) [15] and Re(001) [18].

Potassium gratings were generated at absorbed laser power densities between 1 and 3.5 MW/cm² (the measured reflectivity of Ru(001) at 1.064 μm is 0.75). Monitoring high order SH-diffraction peaks from such coverage grating is the signature of its formation [1,2]. The SH-diffraction spectra obtained from this range of LITD power densities lead to gradual widening of the ejected troughs as laser power increases. This results in changing the diffraction pattern by increasing the relative intensity of the first to zero order diffraction peaks. At power densities above 3 MW/cm², the wider potassium desorbing stripes lead to an effective

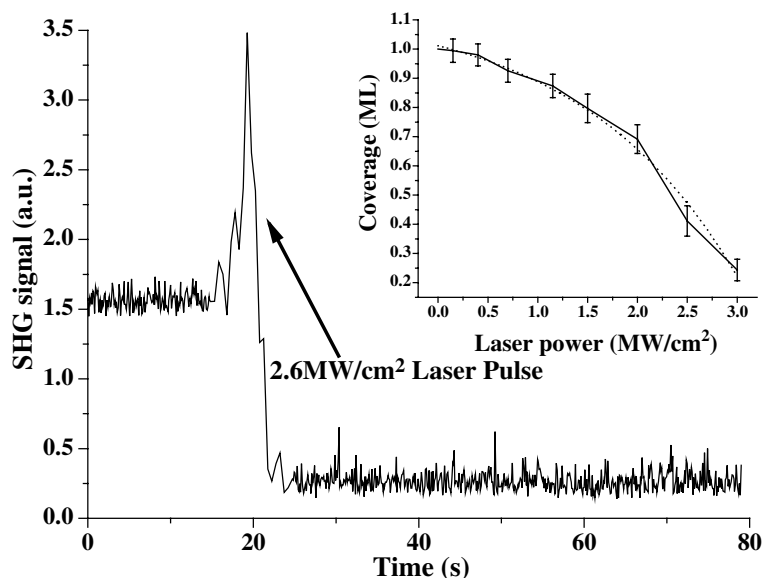


Fig. 2. SHG intensity from 1 ML potassium on Xe: Before, during and after a single laser-desorption pulse at power density of 2.6 MW/cm². K coverage after the pulse, determined by calibrated SH-TPD, was 0.4 ML. Inset: Potassium coverage remaining on the surface after a single laser pulse hit 1 ML K on 60 ML Xe, as function of laser power density. The coverage is determined by the zero order SHG signal before and during SH-TPD. The dashed line represents an exponential fit.

smoothing of the density modulation, thus strongly attenuating the zero, and therefore also higher order SH diffracted signals. The optimal xenon buffer layer assisted potassium grating formation (in terms of SH-diffraction order peak intensities) was obtained at absorbed laser power density of 2 MW/cm².

SH diffraction spectra recorded from potassium gratings are shown in Fig. 3. The diffraction peak intensities are stable, as long as the sample temperature is cold enough to avoid substantial multilayer xenon desorption, namely below 35 K. The absence of any Xe diffusion has been confirmed by optical linear diffraction from clean Xe grating [21]. Further shielding of the metallic patterns from background gases over several hours was obtained, by covering the potassium grating by another layer of xenon. Vacuum impurities, in particular CO, are known to form complexes with potassium, which result in significant quenching of the SHG signal and the corresponding diffraction peaks obtained from coverage grating [22]. The onset for grating formation at laser power densities described above requires a minimum xenon

layer thickness of 2 ML. For all buffer layer thicknesses up to 60 ML, the zero order diffraction peak intensity, that reflects the total potassium coverage, is the same within 10%. In the xenon coverage range of 2–20 ML xenon, increasing the buffer layer thickness tends to change the grating shape into a deeper profile, as deduced from Fourier analysis of the diffracted peak intensities. This is demonstrated in Fig. 4. At layer thicknesses above 20 ML, the removed stripes become somewhat narrower, as indicated by the ratio of the diffracted peak intensities to the zero order reflected SH signal. Lateral heat diffusion, insignificant in the case of metallic substrates, is expected to be significant in physisorbed species like noble gases. Further experiments and analysis are needed in order to better understand the behavior and spatial patterning as the xenon thickness increases.

In order to demonstrate the applicability of our patterning method for strongly bound species, coverage gratings were generated at several initial potassium film thicknesses, from 0.3 to 5 ML, at a Xe buffer layer thickness of 20 ML. Diffraction

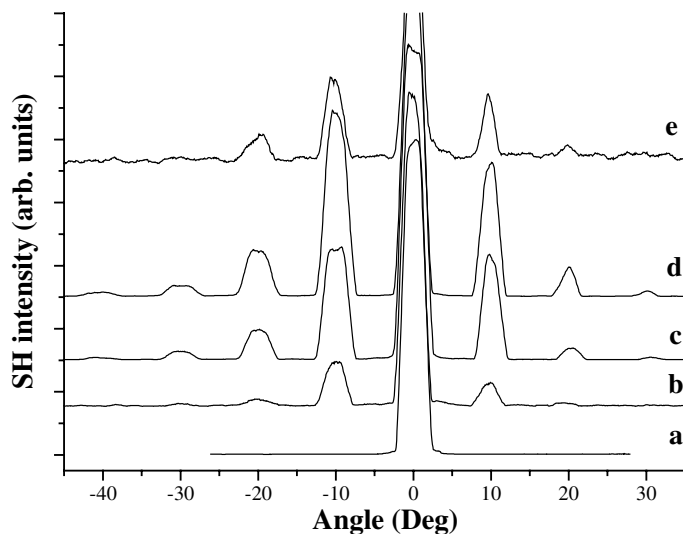


Fig. 3. SH diffraction intensities from potassium coverage grating on a Xe buffer layer, normalized to the zero order SH intensity. (a) deposition of K on a previously prepared coverage grating of 1 ML Xe (laser power density of 4 MW/cm^2), see text; Other diffraction spectra are due to potassium deposited on 20 ML Xe prior to LITD grating formation at 20 K. Laser power density of 2 MW/cm^2 was used throughout for the grating formation: (b) 0.3 ML; (c) 1 ML; (d) 5 ML; (e) 1 ML potassium after annealing the surface to 100 K to evaporate the Xe.

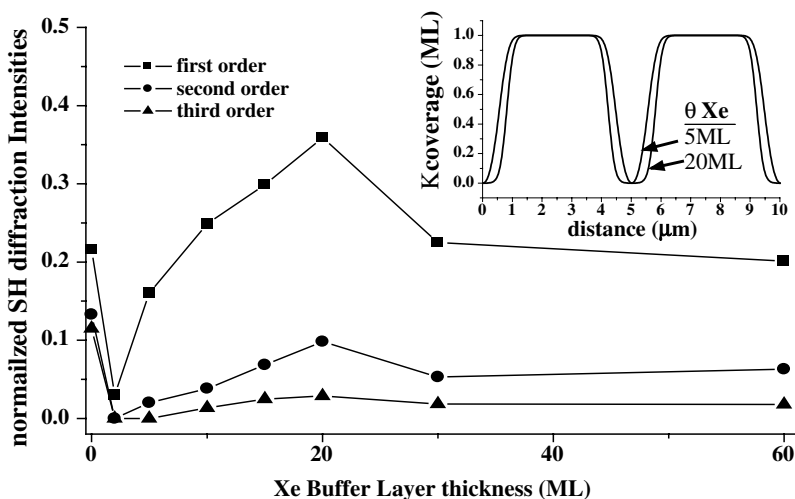


Fig. 4. First, second and third order SH-diffraction peak intensities, normalized to the zero order intensity, as a function of the Xe buffer layer thickness. Laser power density was 2 MW/cm^2 . The zero order peak intensity was constant within 10%. For grating formation of K directly bound to Ru(001) surface (0 ML buffer layer thickness) laser power density of 10 MW/cm^2 was necessary. Inset: Coverage grating profiles as calculated via Fourier analysis of the diffraction peak ratios, at the indicated Xe layer thickness.

spectra are shown in Fig. 3. Grating of 0.3 ML potassium directly adsorbed on Ru(001) is impossible to form by employing laser power

densities below the onset of surface damage (15 MW/cm^2). The strongly bound grating is demonstrated by the diffraction spectrum shown in Fig.

3(b) for a potassium film of 0.3 ML. The 5 ML potassium example, Fig. 3(d), serves to demonstrate potential practical application of the method to form thicker, more realistic conducting wires.

As a further check of the results obtained from our method, we have tested a patterning procedure proposed by Williams et al. [10]. These authors have introduced a technique based on laser-desorption of a xenon film as a template for hydrogen patterning on Si(1 1 1). In their case the species to be patterned were deposited over pre-patterned Xe layer. Our check of the above method started by making a coverage grating within the clean Xe films, and only subsequently potassium was evaporated on top. No diffraction spectrum could be obtained for any Xe thickness or laser power density, prior to or after slow removal of the remaining Xe: Only the zero order SHG signal that reflects the total potassium coverage could be detected, as shown in Fig. 3(a). This is not too surprising in view of the similar sticking of potassium (and most other metals) expected on both the Xe covered and the bare areas of the Ru(001) substrate, which lead to homogeneous, non-patterned potassium coverage.

The metallic adsorbate grating is stable and can be conserved after slowly desorbing the buffer layer at 80 K. This can be verified by the SH dif-

fraction spectrum obtained following the annealing procedure, as shown in Fig. 3(e). The SH diffraction pattern resembles that obtained from potassium grating on top of the xenon layer, Fig. 3(c). One may conclude that slow desorption of the Xe physisorbed buffer layer does not significantly modify the metallic potassium adsorbate grating profile, and that the potassium grating is practically kept intact upon slow xenon removal. The overall intensity of the SH diffraction peaks following Xe removal is, however, reduced. The intensity ratio of the zero, first and second order diffraction peaks, on the other hand, are practically the same as those obtained from potassium grating on top of the Xe buffer layer. This can be explained by the BLAG mechanism introduced by Weaver and coworkers [6–9]. Desorption of the xenon buffer layer near 50 K (multilayer) leads to an abrupt drop of the zero order SHG signal, as shown in Fig. 5. Gradual migration of potassium atoms or small clusters towards the ruthenium surface as the Xe atoms are desorbing, is associated with nucleation and growth of the metallic layer as large particles or clusters. This aggregation process results in reducing the surface area of the potassium, therefore leading to the abrupt decrease of the SH signal. By further heating the sample, SHG regains its intensity to the typical SH

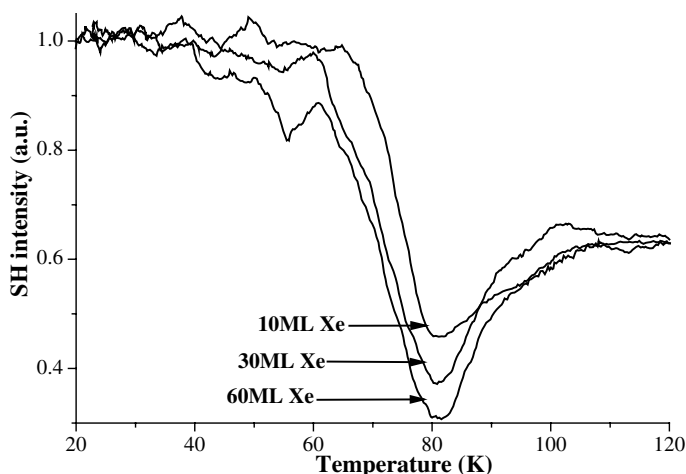


Fig. 5. SH-TPD of 1 ML K/Xe/Ru(001) at the indicated Xe layer thickness. Xenon desorbs at 45–80 K, allowing “soft landing” of metallic K clusters on the Ru surface. Signal attenuation is proportional to the buffer layer thickness. Further heating lead to diffusion of those aggregates, and enhancement of the SHG signal to its typical value on the Ru surface.

response obtained from clean ~ 0.9 ML potassium on the Ru(001) surface. This is probably a result of clusters wetting, therefore recovering the original surface area of potassium on top of the Ru(001) surface. It is reasonable to assume that the metallic lines that form the potassium coverage grating consist of high density potassium clusters formed by the BLAG method.

3. Conclusions

In conclusion, we have developed a procedure for spatial patterning of metallic (or any other strongly interacting species) adsorbates on surfaces utilizing physisorbed buffer layer assisted laser patterning technique. Low laser power densities, required for grating formation, prevent any surface damage. The technique presented here is potentially an attractive alternative method for the deposition of periodic and more complex spatial patterns of conducting wires at widths well below the current limits. This may become a novel future technological pathway since it is a clean UHV based procedure, thus faster and more efficient than wet photo-lithographical techniques that currently dominate in the microelectronics industry. Based on Bragg law, a grating period is given by $\omega = \lambda/2 \sin \theta$, therefore by varying the LITD wavelength to the UV range (e.g. fourth harmonic of a Nd:YAG laser at 266 nm) and angle of incidence to 45° , one can obtain a grating period of $0.19 \mu\text{m}$. Increasing the laser power density, conducting wires can be produced at widths that are 20–25% of the grating period. Consequently, using our method, conducting wires can potentially be patterned that are 5 mm long and less than 30 nm wide. This may be expressed in terms of aspect ratio of more than 10^5 . In Fig. 6, simulated grating patterns are shown of the conducting stripes on top of Xe buffer layer as a function of laser power density for the above laser parameters. The simulations are based on standard LITD process [4,16,21] using desorption kinetic parameters of Xe on Ru(001), as discussed above.

Further developments of the method will include studying different buffer layer materials, which can be used at liquid nitrogen, rather than

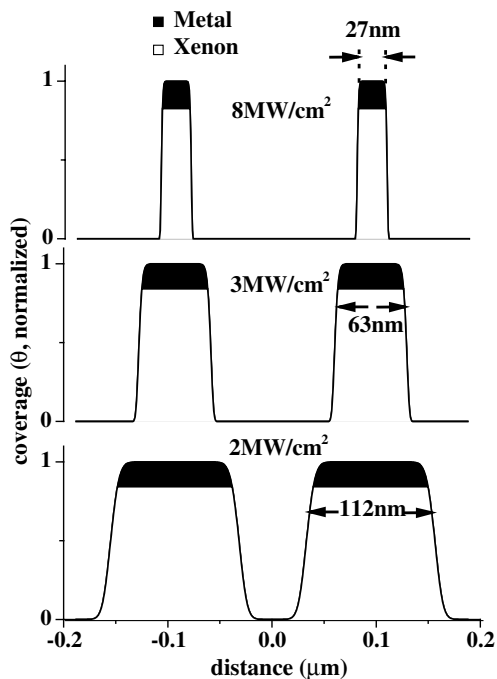


Fig. 6. Simulated LITD grating patterns of potential metallic stripes on top of Xe layers before annealing. For the simulations we used Xe LITD, laser wavelength and angle of incidence parameters as described in the text.

liquid helium temperatures and varying the chemical nature of the film to be patterned. Finally, the use of buffer molecules that would be chemically active with the desired adsorbate is of great interest as well.

Acknowledgements

This work was partially supported by a grant from The US–Israel Binational Foundation and the Israel Science Foundation. The Farkas center is supported by the Bundesministerium für Forschung und Technologie and the Minerva Gesellschaft für die Forschung mbh.

References

- [1] X.D. Zhu, Th. Rasing, Y.R. Shen, Phys. Rev. Lett. 61 (1988) 2883.
- [2] X.D. Xiao, Y. Xie, Y.R. Shen, Surf. Sci. 271 (1992) 295.

- [3] R. Gomer, *Rep. Prog. Phys.* 53 (1990) 917.
- [4] D. Burgess Jr., P.C. Stair, E.J. Weitz, *J. Vac. Sci. Technol. A4* (3) (1986) 1362.
- [5] Z. Rosenzweig, M. Asscher, *J. Chem. Phys.* 96 (5) (1992) 4040.
- [6] J.H. Weaver, G.D. Waddill, *Science* 251 (1991) 1444.
- [7] L. Huang, S.J. Chey, J.H. Weaver, *Phys. Rev. Lett.* 80 (1998) 4095.
- [8] V.N. Antonov, J.S. Palmer, A.S. Bhatti, J.H. Weaver, *Phys. Rev. B* 68 (2003) 205418.
- [9] Ch. Haley, J.H. Weaver, *Surf. Sci.* 518 (2002) 243.
- [10] P.W. Williams, G.A. Reider, L.P. Li, U. Höfer, T. Suzuki, T.F. Heinz, *Phys. Rev. Lett.* 79 (1997) 3459.
- [11] M. Baumer, H.J. Freund, *Prog. Surf. Sci.* 61 (1999) 127.
- [12] C.R. Henry, *Surf. Sci. Rep.* 31 (7/8) (1998) 231.
- [13] (a) S.C. Street, C. Xu, D.W. Goodman, *Annu. Rev. Phys. Chem.* 48 (1997) 43;
(b) H.-J. Freund, *Angew. Chem. Int. Ed. Eng.* 36 (1997) 452.
- [14] W. Zhao, G. Kerner, M. Asscher, M. Wilde, K. Al-Shamry, H.-J. Freund, V. Staemmler, M. Wieszowska, *Phys. Rev. B* 62 (11) (2000) 7527.
- [15] G. Kerner, I.M. Danziger, W. Zhao, M. Asscher, in: M. Tringides, Z. Chevoj (Eds.), *NATO Advanced Research Workshop on Collective Surface Diffusion Coefficients Under Non-Equilibrium Conditions*, Kluwer Academic Publishers, Dordrecht, 2000.
- [16] H. Schlichting, D. Menzel, *Rev. Sci. Instrum.* 64 (7) (1993) 2013.
- [17] H.P. Cheng, U. Landman, *Science* 260 (5112) (1993) 1304.
- [18] R.W. Verhoef, W. Zhao, M. Asscher, *J. Chem. Phys.* 106 (22) (1997) 9353.
- [19] W. Zhao, R.W. Verhoef, M. Asscher, *J. Chem. Phys.* 107 (1997) 5554.
- [20] H.W.K. Tom, C.M. Mate, X.D. Zhu, J.E. Crowell, Y.R. Shen, G.A. Somorjai, *Surf. Sci.* 172 (1986) 466.
- [21] G. Kerner, M. Asscher, submitted.
- [22] W. Zhao, M. Asscher, *Surf. Sci.* 429 (1999) 1.